Polymer Chemistry

Accepted Manuscript

ROYAL SOCIETY OF CHEMISTRY

www.rsc.org/polymers

Journal Name

ARTICLE

Programmable self-assembly of cystamine-block copolymer in response to pH and progressive reduction-ionization-oxidation

Received 00th January 20xx,
Accepted 00th January 20xx

DOI: 10.1039/x0xx00000x

www.rsc.org/

Hui Shi,[a,†] Kaiyi Zhou,[a,†] Qiuping Yu,[a] Zhigang Cui,[a] Yanyan Jiang,[a] Xinhua Lu[a] and Yuanli Cai[a,*]

Direct aqueous synthesis and programmable self-assembly and reconstructions of a well-defined reactive cystamine-block copolymer in response to aqueous environment, such as air and solution pH, are presented in this article. A variety of well-defined poly(cystamine methacrylamide hydrochloride) (PCysMA) and copolymers with 2-hydroxypropylmethacrylamide (HPMA) and 2-aminoethylmethacrylamide hydrochloride (AEMA) can be achieved *via* a fast and well-controlled aqueous RAFT under visible light irradiation at 25°C. PHPMA-*b*-PCysMA assembles into spherical PCysMA-core micelles upon NH_3^+-to-NH_2 conversion. Moreover, progressive reactions in PCysMA block, including reduction, ionization and oxidication, can be induced stepwise by reduction in argon gas saturated acidic water, exposure to air and stepwise alkalization. These reactions lead to stepwise conversion of intermolecular interactions from electrostatic repulsion (ionized PCysMA block) into hydrogen-bonding association (reduction-generated thiol-block), electrostatic repulsion (as-ionized thiolate-block), and hydrophobic cross-linking (oxidation-generated disulfides), leading to programmable self-assembly and reconstruction of a water-soluble block copolymer into compound-encapsulated nanowires, compound-released nanowires, shortened nanorods/spheres, swollen nanowires, nanorods, and branched nanowires/networks. All the phase transformations stem from environment-labile reaction complexity of CysMA unit, and hold potentials in biological and other emerging fields.

Introduction

Stimuli-responsive polymer materials represent a forefront of functional materials.[1, 2] These polymers are positioned to make significant impact in the biomedical,[3, 4] self-healing,[5] and other fields.[6] As emerging stimuli-responsive polymers, the reactive polymers have unique sensitive characters.[7] These polymers served as media-sensitive precursors toward various functional materials with same chain lengths without tedious synthesis of unique monomers,[8-11] thus are facile to tune their functions from a single parent polymer.[12, 13]

Redox-mediated self-assembly of disulfide-based polymers is effective in controlled drug/gene delivery,[14-17] self-healing,[18] and nanoparticle modification.[19, 20] The reversible conversion or exchange was powerful in complex functional systems.[21, 22] Macro-cyclization was achieved via reversible reactions within peptides.[23] Thiol–ene click chemistry is a powerful tool in bio-conjugation, surface modification and hydrogelation.[12, 13, 24, 25] The reversibility was also utilized for inter-conversion between miktoarm stars.[26] Another type of important reactive polymers is NH_2-based poly(L-lysine)s[27] and derivatives.[28] They served as non-viral vectors in gene delivery typically by Narain and other groups.[29] Polymeric NH_2-motifs can be ionized into NH_3^+ ions, and thus assembled into vesicles through complexation with an oppositely-charged block copolymer.[30, 31] Reactivity of NH_2-motifs also enables self-assembly.[32] Our recent results have demonstrated that NH_2-block copolymers can be used as the precursors in a programmable self-assembly *via* dynamic imine conversion and metal coordination.[33, 34]

Recent advances in controlled radical polymerization have boosted the well-controlled synthesis of reactive polymers. Zhao[35] and Oh[25] synthesized the disulfide-containing block copolymers via atom transfer radical polymerisation (ATRP). Reversible addition-fragmentation chain transfer[36, 37] (RAFT) radical polymerisation is superior to ATRP in terms to synthesis of the reactive polymers that consist of the motifs that enable coordination with metal ions. Armes[38] synthesized disulfide-branched copolymers in organic solvent. Cystamine-functional block copolymer was also obtained by RAFT synthesis and then reaction with cystamine.[26] Fulton[39] described RAFT synthesis of statistic copolymers that contained pyridyldisulfide moieties. All these syntheses proceeded in hot solutions typically at 70°C. Obviously, room-temperature aqueous synthesis is desirable in respect to ensuring the intact reactive moieties.

Nano-objects with environment-labile reaction complexity have emerged as advanced stimuli-responsive smart materials. However, direct aqueous synthesis is still challenging. Langer[40] showed amazing superiority of a cystamine-containing poly(β-aminoester) in gene delivery, whereas the synthesis was time-

[a] *Jiangsu Key Laboratory of Advanced Functional Polymer Design and Application, Suzhou Key Laboratory of Macromolecular Design & Precision Synthesis, College of Chemistry, Chemical Engineering and Materials Science, Soochow University, Suzhou 215123, China. E-mail: ylcai@suda.edu.cn; Tel & Fax: +86-512-65884419*
[†] The authors contributed equally to this work.
Electronic Supplementary Information (ESI) available: Synthesis of PHPMA macro-CTA; ^{1}H NMR of CysMA, reaction solutions; ^{1}H NMR and SEC of purified samples; CysMA/AEMA copolymerisations; CysMA & PHPMA-*b*-PCysMA titrations. See DOI: 10.1039/x0xx00000x

consuming and less effective (*via* addition of 2-pyridyldithioethylamine (PDA) with diacrylates followed by exchange with mercaptoethylamine). High temperatures and excess PDA over diacrylate could induce the significant cross-linking. Thus, only oligomers with MW<4 kDa could be obtained. Moreover, their molecular weights were ill-controlled due to intrinsic nature of step-growth polymerisation. However, well-defined cystamine-polymer seems indispensable in order to unveil environment-labile behaviours of such a unique reactive polymer.

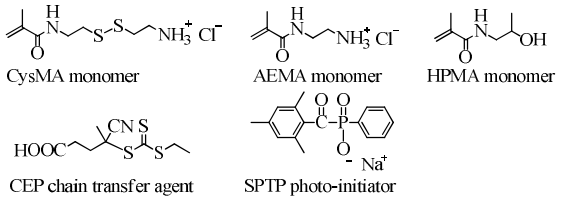

Chart 1 chemical structures of CysMA, AEMA, HPMA, CEP and SPTP used in this article.

Herein, we report direct aqueous synthesis of well-defined cystamine-(co)polymers under visible light irradiation at 25°C. Cystamine methacrylamide hydrochloride (CysMA, see Chart 1) was designed, and the aqueous RAFT synthesis (including block and statistic copolymerisation with HPMA and/or AEMA) was studied using ^{1}H NMR spectroscopy and size exclusion chromatography (SEC). Moreover, environment-labile programmable self-assembly and reconstructions of a well-defined cystamine-block copolymer, PHPMA-*b*-PCysMA were studied by acid-base titration, ^{1}H NMR, dynamic light scattering (DLS), aqueous electrophoresis, and transmission electron microscopy (TEM).

Experimental

Materials

HPMA,[41] AEMA,[42] CEP,[43] SPTP[44] were synthesized according to literature procedures. Poly(2-hydroxypropylmethacrylamide) (PHPMA) was synthesized (see details in Electronic Supporting Information, ESI, Fig. S1), and used as a macromolecular chain transfer agent (macro-CTA). Cystamine dihydrochloride was purchased from TCI; methacryloyl chloride and DTT were from Sigma-Aldrich; deuterium oxide (D_2O, 99.8%D), deuterchloric acid (DCl, 99.5%D, 20% in D_2O) and sodium deuteroxide (99.5% D, 40% in D_2O) from J&K; triethylamine (TEA), butoxyethanol (BOE), methanol, 2-propanol, hydrochloric acid and NaOH were from Sinopharm; these agents were used as received. Deionized water was obtained from AQUELX 5 Millipore.

Synthesis of cystamine methacrylamide hydrochloride (CysMA)

Cystamine dihydrochloride (79.1 g, 0.35 mol) and NaOH (18.8 g, 0.47 mol) were dissolved in the mixture of methanol (190 mL) and water (170 mL) in a 500-mL flask. Methacryloyl chloride (18.83 g, 0.18 mol) was added under stirring overnight at -20°C. The solution was adjusted to pH 2.0 using 5.0 M hydrochloric acid, and rotary evaporated and lyophilized. The solids were extracted using 2-propanol, and recrystallized from 2-propanol at -20°C. Drying under reduced pressure afforded white solid product. Yield: 18.9 g, 31.5%. ^{1}H NMR (in D_2O, δ, ppm): 5.7 and 5.5 (2H, C**H**$_2$=C), 3.6 (2H, C**H**$_2$NH$_3^+$), 3.4 (2H, CONHC**H**$_2$), 3.0 (4H, C**H**$_2$S-SC**H**$_2$), and 2.0 (3H, CH$_2$=CC**H**$_3$).

Visible light irradiation

A 400-W mercury lamp was selected, and JB400 filters were used to remove UV irradiation at λ_{em} < 400 nm and decrease to I_{420nm}=0.25 mW/cm^2 (ca. 5% of solar irradiation in May in East China). The visible light intensity was determined using a UV-A radiometer equipped with λ=420 nm detector.

Aqueous RAFT synthesis under visible light irradiation

A typical protocol is as follows: CysMA (506.0 mg, 1.97 mmol), CEP (2.6 mg, 9.89 μmol), and SPTP (0.8 mg, 2.58 μmol) were dissolved in BOE/water (20:80, 0.51 g) in a 10-mL flask. After bubbled with argon gas for 40 min, the solution was irradiated with visible light at 25°C. Samples were taken at different time points for ^{1}H NMR and SEC studies. After irradiation for 2 h (^{1}H NMR: 94% conversion), reaction was ceased upon exposure to air and addition of hydroquinone inhibitor. The final solution was dialyzed against water using dialysis membrane (MWCO= 1.0 kDa), and lyophilized. ^{1}H NMR: PCysMA$_{198}$; SEC: M_n=59.2 kDa, M_w/M_n= 1.12. Procedures for the synthesis of P(AEMA-*stat*-CysMA), PHPMA-*b*-PCysMA and PHPMA-*b*-P(AEMA-*stat*-CysMA) were the same as above, except for the use of both CysMA and AEMA for the statistic structures, and a PHPMA macro-CTA for the block or block-statistic structures.

One-pot iterative synthesis of PAEMA-*b*-PCysMA block copolymer

CysMA (1.05 g, 4.10 mmol), CEP (10.8 mg, 41.1 μmol), SPTP (3.2 mg, 10.3 μmol) were dissolved in BOE/water (20:80, 1.0 g) in a 10-mL flask. The solution was bubbled with argon gas for 40 min. After irradiation for 2.5 h (^{1}H NMR: >98% conversion), light was shielded, and sample was taken. Argon gas-saturated AEMA (0.677 g in 1.373 g water, 4.10 mmol) was added. The solution was irradiated for 1 h (^{1}H NMR: 66% conversion). The sample was obtained by dialysis and lyophilisation. ^{1}H NMR: PAEMA$_{67}$-*b*-PCysMA$_{98}$; SEC: M_n=53 kDa, M_w/M_n=1.13.

^{1}H NMR spectroscopy

^{1}H NMR spectra were recorded on an INOVA 400 MHz NMR.

Size exclusion chromatography (SEC)

Molecular weight (M_n) and polydispersity index (PDI, M_w/M_n) were determined on a PL-GPC220 integrated system equipped with a refractive index detector and a set of columns (2×PLGel MIXED-B+1×PLGel MIXED-D). HPLC-grade DMF that contained 10.0 mM LiBr was filtered prior to use as eluent. Poly(methyl methacrylate) (PMMA, Agilent, 7.36-2136.0 kDa) were used for calibration. All the calibration and analysis were carried out at a 1.0 mL min^{-1} flow rate at 80°C. To avoid absorption onto the column materials, the polymeric primary amine moieties were reacted with methyl acrylate under literature procedures.[45, 46]

Acid-base titration

Typically, PCysMA$_{96}$ (15.0 mg) was dissolved in water (3.0 mL). The solution was acidified by 5.0 M hydrochloric acid, and then

titrated using a 1.0 M NaOH solution at 25°C. The solution pH values were recorded using a Denver UB-7 digital pH-meter.

Aqueous electrophoresis

Zeta potential (ζ) parameters of the particles were determined by aqueous electrophoresis on Malvern Zetasizer Nano-ZS90.

Dynamic light scattering (DLS)

DLS studies were performed on a Brookhaven BI-200SM setup equipped with 22-mW He-Ne laser (λ=633 nm), BI-200SM goniometer and BI-TurboCorr digital correlator. The solution was controlled at 25 ± 0.02°C using BI-TCD controller. The scattered light at 90° was recorded. The intensity-average hydrodynamic diameters (D_h) and dispersity (μ_2/Γ^2) were determined by the use of cumulants analysis in CONTIN routine.

Transmission electron microscopy (TEM)

TEM images were obtained using Hitachi HT7700 transmission electron microscope at accelerating voltage of 120 kV. As-cast solution on carbon-coated copper grid was lyophilized prior to the measurement.

Results and discussion

Aqueous RAFT synthesis under visible light irradiation at 25°C

Our recent results[47] demonstrate visible light irradiation can induce ultrafast aqueous RAFT polymerisation at 25°C, and the reaction start or suspend immediately by turning on/off visible light,[42, 48, 49] such that the degree of polymerisation (DP) can be controlled in chain extension.[49] This synthesis technique was employed for direct synthesis of well-defined cystamine-based polymers. SPTP was obtained through a patented procedure.[44] It is weak acid at a pKa of 6.50, and has broad n→π* transition band at λ_{max}=371 nm.[49] Its lithium salt was used for the photosynthesis of living cell scaffolds,[50] extracellular mimics[51] and hydrogels.[52] Our results revealed effective aqueous RAFT upon using SPTP initiator under visible light irradiation at 25°C.[49, 53]

CysMA monomer was obtained via reaction of cystamine dihydrochloride with methacryloyl chloride in methanol/water in presence of sodium hydroxide at -20°C. This NH_3^+/disulfide-functionalized monomer shows a pKa=9.2, whose NH_3^+-motifs start to deionize above pH 5.1 and fully convert into reactive NH_2 groups above pH 10.9 (Fig. S2). Accordingly, the aqueous RAFT synthesis proceeded in acidic water at pH 3.0, such that aminolysis of CEP chain-ends[54] can be circumvented and SPTP was converted into non-ionic acid.[49] CEP (Chart 1) was used to mediate RAFT process. Based on the previous results,[43, 54] CEP could mediate aqueous RAFT of methacrylamide monomers. The syntheses proceeded in 2-butoxyethanol/water (20:80), so that CEP was dissolved and electrostatic repulsion of ionized CysMA and growing-chains (which may slow down the chain propagation[55]) could be effectively minimized. These reactions started at $[CEP]_0/[SPTP]_0$=4 under weak visible light irradiation (I_{420nm}=0.25 mW/cm^2) at 25°C. The monomer conversions were monitored by ^{1}H NMR studies of the samples taken at different irradiation time (Fig. S3).

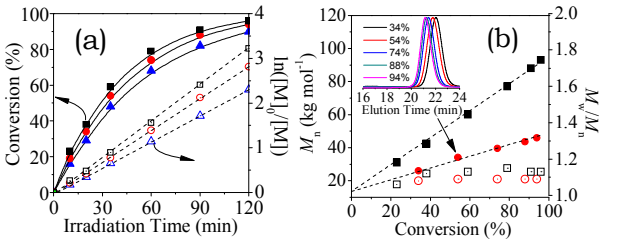

Fig. 1 (**a**) the polymerisation kinetic plots at a $[CysMA]_0$=1.95 M upon the variation of $[CysMA]_0/[CEP]_0$ from 100 (▲) to 200 (●) and 300 (■); (**b**) the variation of molecular weights (solid) and dispersity (hollow) upon polymerisation at $[CysMA]_0/[CEP]_0$=200 (●) and 300 (■) (*Insert*: SEC trace shift during polymerisation at $[CysMA]_0/[CEP]_0$=200).

As shown in Fig. 1a, visible light irradiation induced an effective RAFT to >90% conversions within 2 h over targeted degree of polymerisation (DP_{target}, $[CysMA]_0/[CEP]_0$) of 100-300, and the growing-chain radicals maintained constant (indicated by linear increase of semi-logarithmic kinetic plots), with the apparent propagation rate constants (k_{app}, indicated by the plot gradients) increased with DP_{target}. Moreover, as illustrated in Fig. 1b, their SEC traces are unimodal and symmetrical, and shift to high molecular weights. Their molecular weights (M_n) increased linearly with monomer conversions, and their molar mass distributions are very low, i.e. around an M_w/M_n=1.10. Moreover, their reactive CysMA units maintained intact after dialysis and then lyophilisation, as judged by ^{1}H NMR and SEC results (Fig. S4). These results suggest that their disulfide/NH_3^+ moieties were stable under such mild aqueous conditions.

Aqueous RAFT synthesis of PCysMA-based block copolymers

To illustrate, a well-defined $PHPMA_{90}$ macro-CTA was selected, which was also synthesized by aqueous RAFT using CEP chain transfer agent and SPTP initiator under visible light irradiation at 25°C (ESI). This chain-extension experiment proceeded at $[CysMA]_0$=1.30 M, $[CysMA]_0/[PHPMA_{90}]_0$=100. ^{1}H NMR results indicate a 60% conversion after 1 h of irradiation. The purified sample was obtained after dialysis and lyophilisation.

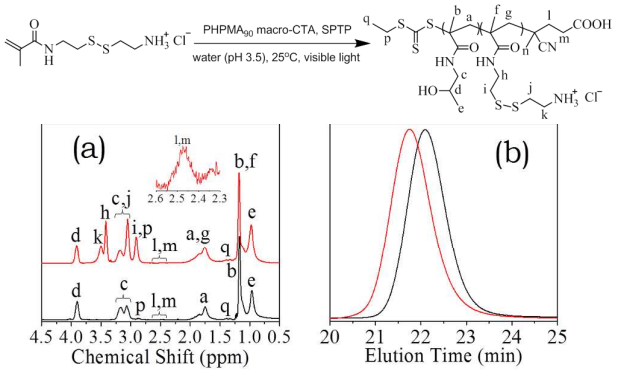

Fig. 2 (Top) schematic illustration for synthesis of PHPMA-*b*-PCysMA via macro-CTA method; (bottom) ^{1}H NMR spectra (a) and SEC traces (b) of PHPMA macro-CTA (*black*) and the chain-extended PHPMA-*b*-PCysMA (*red*).

As shown in bottom of Fig. 2a, $I_b/I_{b+e}/I_c/I_d$ was assessed to be 2/6/2/1, in agreement with the proton ratio of PHPMA

macro-CTA. Integral signals *l*, *m* within CEP chain-ends were selected to determine the degree of polymerization (DP_{HPMA}) according to $DP_{HPMA}=(4\times I_d)/I_{l+m}$, in which I_d is the integral signal C**H**(CH_3)OH in HPMA units. DP_{HPMA} of 90 was thus assessed, i.e. $PHPMA_{90}$ macro-CTA. As shown in top of Fig. 2a, the signals of both blocks are completely detected in acidic deuterium oxide. Moreover, the integral ratio $I_{h+k}/I_{i+j+c}/I_{b+e+f}/I_d$ equals 3:5:8.3:1 or $I_{h+k}/I_{i+j}/I_f$ equals 4:4:3, which indicate that the disulfide/NH_3^+ moieties within PCysMA block maintained intact under such polymerisation/purification conditions. Hence, the molecular structure $PHPMA_{90}$-*b*-$PCysMA_{70}$ was determined according to $DP_{HPMA}=(4\times I_d)/I_{l+m}$ and $DP_{CysMA}=(4\times I_{h+k})/I_{l+m}$. As shown in Fig. 2b, after chain extension, the SEC analysis indicated an increase in molecular weight from M_n=28.2 kDa of $PHPMA_{90}$ macro-CTA to M_n=37.6 kDa of as-obtained $PHPMA_{90}$-*b*-$PCysMA_{70}$ sample.

To illustrate effectiveness of this aqueous RAFT, iterative reaction was explored for one-pot synthesis of PCysMA-block copolymer, in which NH_3^+-based 2-aminoethylmethacrylamide hydrochloride (AEMA, Chart 1)[42] was added in the reaction solution immediately after CysMA monomer was completely polymerized.

^{1}H NMR indicated that 2.5 h of irradiation led to extremely high conversion (>98%) of CysMA monomer, and SEC analysis indicated a low polydispersity index at M_w/M_n=1.10 (Fig. S5). Argon gas saturated AEMA solution was added in the reaction solution, and then irradiated for 1 h. ^{1}H NMR indicated a 66% conversion of AEMA monomer. After dialysis and lyophilisation, a well-defined $PAEMA_{67}$-*b*-$PCysMA_{98}$ copolymer (M_w/M_n=1.13, intact PCysMA block) was obtained, as judged by ^{1}H NMR and SEC (Fig. S6). These results illustrate that the all-NH_3^+-block copolymers can be synthesized by this iterative reaction. Both macro-CTA method and iterative synthesis demonstrate a high efficiency of the unique aqueous RAFT in synthesis of PCysMA-block copolymers.

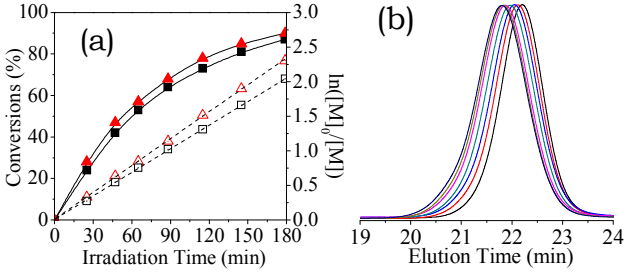

Fig. 3 (a) the kinetic plots for the copolymerization of CysMA (■) and AEMA (▲) at $[AEMA]_0/[CysMA]_0$=0.25, $[monomers]_0$=1.95 M and $[monomers]_0/[CEP]_0$=100; (b) the SEC trace shift with irradiation time (*from left to right*: 25, 47, 65, 88, 115, 145, 179 min.

Synthesis of CysMA-based statistic and block-statistic copolymers

As shown in Fig. 3a, 87% CysMA and 90% AEMA conversions were achieved at $[AEMA]_0/[CysMA]_0$=0.25 after irradiation for 3 h. The linear kinetic plots indicated constant living growing-chain radicals, and AEMA monomer polymerized faster than CysMA ($k_{app,CysMA}$=0.68 h^{-1}, $k_{app,AEMA}$=0.77 h^{-1}). The increase of irradiation time led to the SEC traces shifting to high molecular weight side (Fig. 3b), indicating well-controlled behaviour. The chain propagation at $[AEMA]_0/[CysMA]_0$=4 ($k_{app,CysMA}$=1.34 h^{-1}, $k_{app,AEMA}$=1.52 h^{-1}, Fig S7) proceeded faster than the former, because of the use of AEMA as major co-monomer. Reactivity ratios were thus assessed (r_{CysMA}=0.88, r_{AEMA}=1.16) according to Jaacks Equation (Table S1),[56] suggesting that it is a pseudo-ideal copolymerization (as judged by $r_{CysMA}\times r_{AEMA}$=1.02). Thus, the copolymer have typical statistic structure or P(AEMA-*stat*-CysMA). Further purification afforded well-defined copolymers (Fig. S8). PHPMA-*b*-P(AEMA-*stat*-CysMA) was synthesized upon using a $PHPMA_{90}$ macro-CTA. Block-statistic structures with an adjustable ratio $[AEMA]_0/[CysMA]_0$ over 0.25-4 (Fig S9) was confirmed by the kinetic studies ($r_{CysMA}\times r_{AEMA}$=0.95×1.17=1.11, Table S2). ^{1}H NMR and SEC results confirmed intact molecular structures with M_w/M_n values of 1.13-1.18 (Fig. S10).

Table 1 The structure parameters of cystamine-based (co)polymers

Entry	Molecular Structure [a]	$M_{n,1H\ NMR}$ [a] (kDa)	$M_{n,SEC}$ [b] (kDa)	M_w/M_n [b]
P-1	$PCysMA_{96}$	24.9	37.1	1.10
P-2	$PCysMA_{198}$	51.1	59.2	1.12
P-3	$PCysMA_{303}$	78.0	90.4	1.14
P-4	$PHPMA_{90}$-*b*-$PCysMA_{70}$	36.1	37.6	1.17
P-5	$PAEMA_{67}$-*b*-$PCysMA_{98}$	36.4	53.0	1.13
P-6	P($AEMA_{79}$-*stat*-$CysMA_{19}$)	18.1	34.1	1.13
P-7	P($AEMA_{49}$-*stat*-$CysMA_{46}$)	20.1	35.2	1.16
P-8	P($AEMA_{22}$-*stat*-$CysMA_{82}$)	24.9	37.8	1.15
P-9	$PHPMA_{90}$-*b*-P($AEMA_{77}$-*stat*-$CysMA_{18}$)	31.8	30.8	1.17
P-10	$PHPMA_{90}$-*b*-P($AEMA_{51}$-*stat*-$CysMA_{47}$)	35.0	39.1	1.13
P-11	$PHPMA_{90}$-*b*-P($AEMA_{16}$-*stat*-$CysMA_{78}$)	37.2	44.0	1.18

(a) $M_{n,1H\ NMR}$ and the molecular structures were determined by ^{1}H NMR studies; (b) $M_{n,SEC}$ and M_w/M_n were determined by SEC studies.

As summarized in Table 1, a variety of well-defined CysMA-(co)polymers can be easily synthesized by aqueous RAFT under visible light irradiation at 25°C. The structures can be mediated from homo to block, statistic and block-statistic structures. To our awareness, this is the first time to report direct synthesis of well-defined cystamine-based polymers and the copolymers under such mild aqueous conditions. More importantly, these well-defined cystamine-polymers are ideal materials to unveil their reaction-induced environment sensitive behaviours.

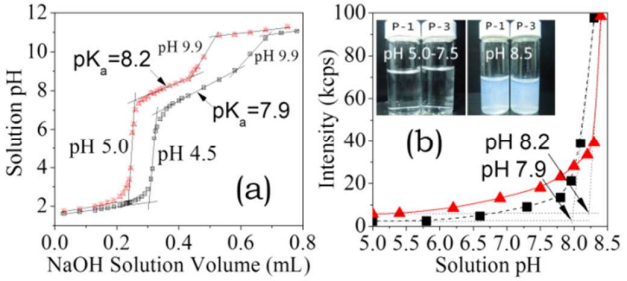

Fig. 4 (a) Acid-base titration plots of $PCysMA_{96}$ (*black*, P-1) and $PCysMA_{303}$ (*red*, P-3); (b) light scattering intensity as a function of the solution pH (*insert*: solution photographs).

Self-assembly of PHPMA-*b*-PCysMA in response to solution pH

$PCysMA_{96}$ and $PCysMA_{302}$ were used to study phase transition in response to alkalization-induced NH_3^+-to-NH_2 conversion. As shown in Fig. 4a, $PCysMA_{96}$ underwent a transition at pH 4.5 to which NH_3^+-to-NH_2 conversion started, a buffer zone at pH 6.9-9.0 (pKa=7.9), and a critical point (pH 9.9) of full conversion. It dissolved into acidic water but precipitated from alkali solution, as judged by transparent-to-turbid transition upon alkalization (Fig. 4b). Moreover, light scattering intensity increased sharply on alkalization to pH 7.9, which suggest sufficient hydrophobic association of disulfide spacers to induce effective dehydration, as judged by ^{1}H NMR (Fig. 5b).

In contrast, $PCysMA_{303}$ shows a pKa=8.2, in which 0.18 mL NaOH solution was consumed over buffer zone (lower than the former, 0.26 mL), suggesting that the ionized CysMA units were partially encapsulated into the precipitates. Its critical solution pH of phase transition (pH 8.2, Fig. 4b) was also higher than that of $PCysMA_{96}$, which confirms that the hydrophobic association induced the encapsulation of ionized CysMA units.

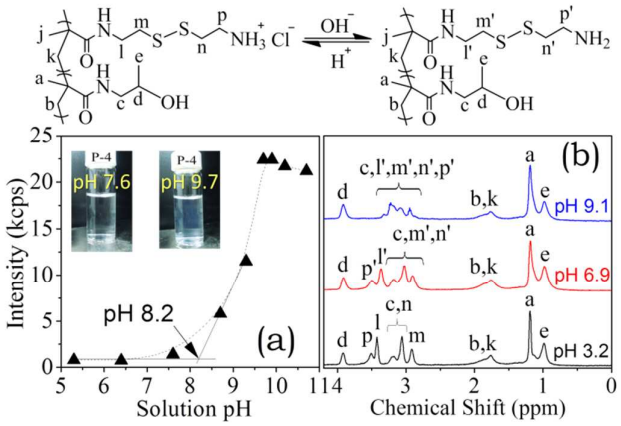

Fig. 5 (a) The variation light scattering intensity of 3.0 mg mL^{-1} of $PHPMA_{90}$-*b*-$PCysMA_{70}$ in water with the solution pH at 25°C (*insert*: solution photographs); (b) ^{1}H NMR spectra of the solutions in deuterium oxide at pH 3.2 (black) and pH 9.1 (red).

$PHPMA_{90}$-*b*-$PCysMA_{70}$ was selected to study pH-responsive self-assembly because the PHPMA block is water-soluble and biocompatible.[34, 41, 49, 57] Indeed, phase transition occurred on alkalization, leading to a transition of transparent solution into light bluish and a sharp increase of light scattering intensity above pH 8.2 (Fig. 5a), higher than its pKa at pH 7.8 (Fig. S11). Moreover, signals *l*, *p* upfield shifted, and $I_{l+m+n+p}/I_d$ (using the signal *d* as internal standard) decreased from 6.0 to 5.3 and 1.5 ($I_{l'+m'+n'+p'}/I_d$) on alkalization from pH 3.2 to 6.9 and 9.1 (Fig. 5b), suggesting that NH_3^+-to-NH_2 conversion induced hydrophobic association and thus dehydration of PCysMA block.

As shown in Fig. 6a, DLS analysis revealed the formation of micelles with intensity-average hydrodynamic diameter (D_h) of 29 nm and low dispersity of 0.047, in which intensity increased to 32 kcps. TEM visualized spherical micelles of as-lyophilized samples with overall sizes of ca. 30 nm (Fig. 6b). Therefore, this block copolymer self-assembled into PCysMA-core micelles. The reaction complexity including high reactivity of NH_2 groups and media-labile disulfide spacers within CysMA unit inside the nano-confined hydrophobic cores provide a general and also versatile platform for the exploring of unique media-sensitive behaviours as recently proposed by Langer and co-workers.[40]

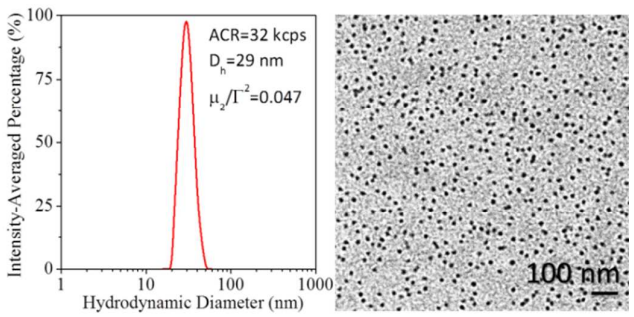

Fig. 6 DLS results of the micelles of $PHPMA_{90}$-*b*-$PCysMA_{70}$ (*left*, 1.0 mg mL^{-1} in water at pH 9.7); TEM image of the as-lyophilized block-copolymer micelles (*right*)

Air/pH-mediated programmable self-assembly and reconstruction

$PHPMA_{90}$-*b*-$PCysMA_{70}$ was dissolved in D_2O, and then adjusted to 3.0 mg/mL and pH 3.5 using a DCl solution (20% in D_2O). Dithiothreitol (DTT, $[DTT]_0/[CysMA]_0$=1.80) was added in the solution. This solution was saturated with inert argon gas and stirred overnight prior to ^{1}H NMR measurement. As shown in Fig. 7, the block copolymer and DTT were stable in the solution at pH 3.5, as indicated by their invariable integral signals. After the mixture was stirred in inert argon atmosphere overnight, the signals *l*, *p* in PCysMA block disappeared, and signals *b*, *k* in the polymer backbones decreased. Moreover, after dialysis to remove small compounds, only the signals in PHPMA block are detected. The results demonstrate that disulfide linkages have been already reduced. The inter-chain interactions evolved from electrostatic repulsion of initially ionized PCysMA block to hydrogen-bonding association of reduction-generated thiol block, leading to full dehydration of the water-soluble block in acidic media.

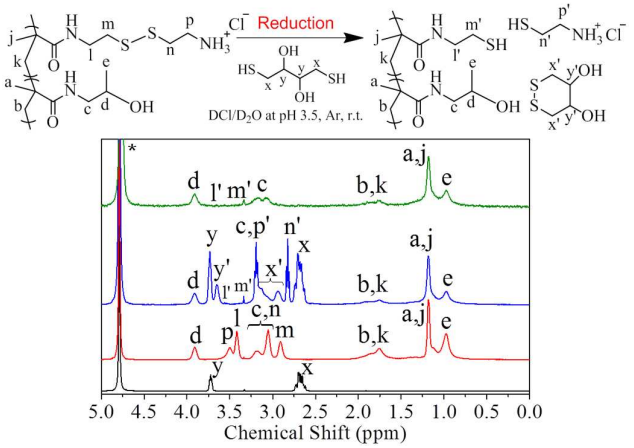

Fig. 7 (*Top*) schematic illustration for reduction reaction of $PHPMA_{90}$-*b*-$PCysMA_{70}$ using DTT in argon gas saturated D_2O at pH 3.5; (*bottom*) ^{1}H NMR spectra of (*from bottom to top*) DTT, the block copolymer, and the reaction solutions of both before/after dialysis.

To illustrate the air/pH-sensitive behaviours, the solution was exposed to air, and separated into several portions. Each portion was adjusted to predetermined pH values using NaOD (40% in D_2O) and stirred at room temperature overnight. As shown in Fig. 8a, $I_{y'+y''}/I_d$ at pH 8.5 equals $I_{y+y'}/I_d$ at pH 3.5 with an increase of $I_{y'}/I_d$ from 2.0 to 4.0 and decrease of I_x/I_d from 6.2 to 2.3 because DTT was oxidized to 1,2-dithiane-4,5-diol,[58, 59] suggesting that the polymeric thiolate ions were air-oxidized faster than the corresponding non-ionic thiols.[58, 60] Moreover, signals *l'*, *m'* attenuated but were still detectable at pH 3.5 and 5.1, suggesting a slight hydration of the units. These signals disappeared at pH 8.5, due to intensive cross-linking caused by as-generated hydrophobic disulfide bonds.[12, 13, 24, 25]

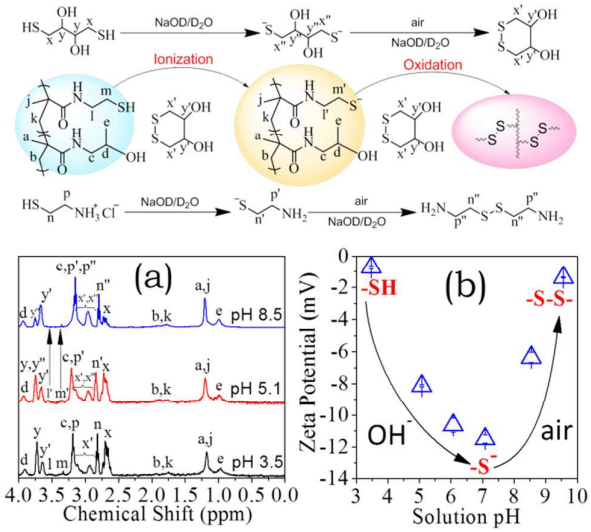

Fig. 8 (*Top*) schematic illustration for air/pH-mediated ionization and oxidation in the solution described in Fig 7; (*bottom*) variable ^{1}H NMR spectra (**a**) and zeta potentials (**b**).

Zeta potential (ζ) parameter represents the surface charge of nanoparticles in relation to the surrounding circumstance.[61] Therefore, inspection of pH-responsive ζ-variation of particles[9, 62-64] allows the convenient discrimination of a charge increase caused by alkalization-ionized polymeric thiolate anions, and also a charge decrease owing to oxidation of thiolate anions into non-ionic disulfides. As shown in Fig. 8b, ζ values are negative over pH 3.5-9.6. It decreases from -0.7 to -11.5 mV upon alkalized from pH 3.5 to 7.1, which confirm ionization of these polymeric thiols. Nevertheless, it increases from -11.5 to -1.4 mV after an increase from pH 7.1 to 9.6, which suggests the air-oxidation of thiolate ions into non-ionic disulfides. This tendency is in good agreement with those in air-oxidation of thiol compounds, [58, 60] in which air-oxidation was remarkably accelerated and only disulfide derivatives could be generated in the alkali aqueous solutions at ambient temperature.

As shown in Fig. 9a, phase separation led to a significant increase of light scattering intensity from 0.78 up to 190.8 kcps after reduction at pH 3.5, and the polymer chains have self-assembled into particles at D_h=164 nm and dispersity of 0.187. Average size and light scattering intensity increased to D_h = 182 nm and 253.1 kcps at pH 5.1 due to release of encapsulated small molecules, but decreased to D_h=81 nm and 99.2 kcps at pH 7.1 due to ionization as judged by a decrease of ζ value (Fig. 8b). However, both the size and intensity increased from D_h= 131 nm and 298.2 kcps to D_h=276 nm and 401.7 kcps after the increase from pH 8.5 to 9.6 (Fig. 9b), because of hydrophobic cross-linking of disulfide bonds formed by air oxidation.[65, 66]

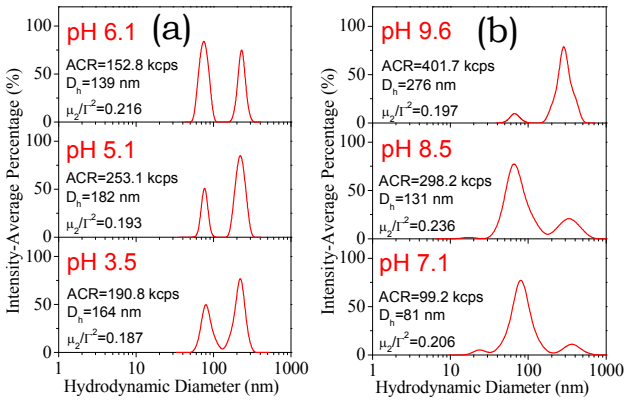

Fig. 9 DLS results of the variation of DTT-reduced $PHPMA_{90}$-*b*-$PCysMA_{70}$ aggregates (Fig. 7) after alkalization to predetermined pH values in air under the conditions of Fig. 8

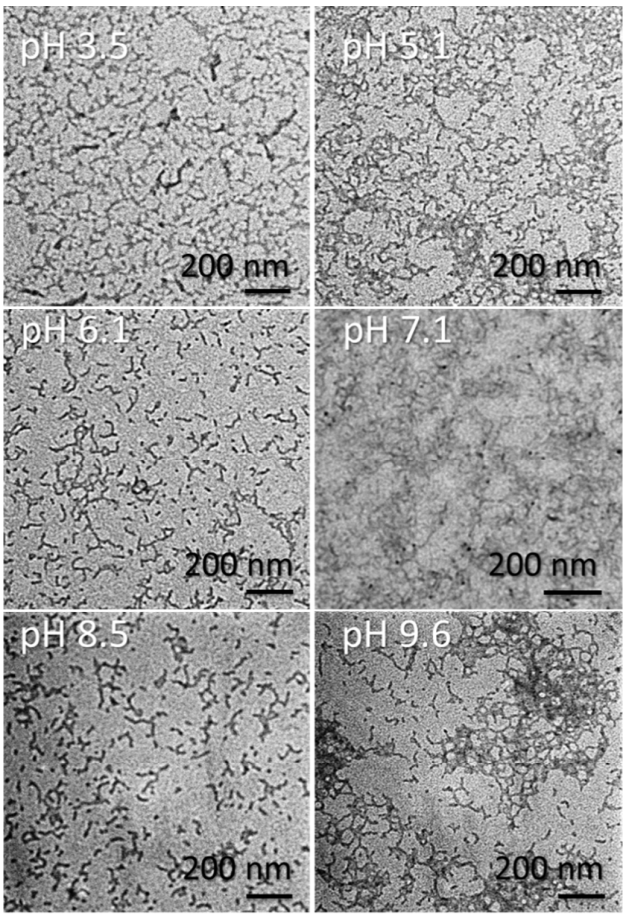

Fig. 10 TEM images of lyophilized samples of as-reduced $PHPMA_{90}$-*b*-$PCysMA_{70}$ solution after adjusted to the predetermined pH values in ambient air and stirred overnight.

As shown in Fig. 10, this block copolymer self-assembled into nanowires after the reduction at pH 3.5. These nanowires became unambiguous at pH 5.1 because of the release of compounds from nanowire cores. The nanowires ruptured into short nanorods and spheres at pH 6.1 due to the electrostatic repulsion interactions.[64] Intriguingly, swollen nanowires still maintained at pH 7.1, in which the solubility was enhanced by increase of as-formed thiolate ions. These results indicate air-oxidation into inter-chain disulfides. Indeed, air oxidation of thiol molecules occurred in neutral aqueous solution.[65, 66] The hydrophobic cross-linking of oxidation-generated inter-chain disulfide bonds were strong enough to maintain nanostructure. Intensified oxidation in alkali solutions resulted in formation of unambiguous nanorods at pH 8.5 and even inter-particle cross-linking into branched nanowires/networks at pH 9.6.

These results demonstrate that these reduction-ionization-oxidation reactions trigger stepwise evolving of intermolecular interactions from electrostatic repulsion of ionic PCysMA block to the hydrogen-bonding association of as-reduced thiol block, electrostatic repulsion of anionic thiolate-block, and finally hydrophobic cross-linking of the air-oxidized disulfide linkages, leading to unique assembly and reconstruction programmable into compound-encapsulated nanowires, compound-released nanowires, shortened nanorods/spheres, swollen nanowires, nanorods and branched nanowires/networks. These resultant nanowires/networks are stable against solution pH, as judged by the constant light scattering intensity and size profiles upon adjusting the solution back and forth over pH 9.6 - 5.1. These unique phase transformations stem from the media-sensitive reaction complexity of CysMA unit. These environment-labile characters opened up a new route toward stimuli-responsive materials important in biological and other emerging fields.[1-5]

Conclusions

This article described direct aqueous synthesis and aqueous environment-labile programmable assembly/reconstruction of a reactive cystamine-block copolymer. To this end, a variety of well-defined PCysMA and copolymers with HPMA/AEMA were synthesized via fast and well-controlled aqueous RAFT under visible light irradiation at 25°C. The pH-induced self-assembly and environment-mediated self-assembly and reconstruction of $PHPMA_{90}$-*b*-$PCysMA_{70}$ were studied using acid-base titration, ^1H NMR, DLS, aqueous electrophoresis and TEM.

The results demonstrated that NH_3^+-to-NH_2 conversion via alkalization induced the phase transition of PCysMA block, and PHPMA-*b*-PCysMA self-assembled into spherical PCysMA-core micelles. Moreover, the progressive reactions, which included reduction, ionization and oxidation, occurred on the reduction in argon gas saturated acidic water, exposure to air followed by stepwise alkalization. The reactions triggered inter-chain interactions evolving from electrostatic repulsion of ionized PCysMA block to hydrogen-bonding association of reduction-generated thiol-block, electrostatic repulsion of ionic thiolate-block, and cross-linking of oxidation-generated hydrophobic disulfide bonds, leading to air/pH-induced programmable self-assembly and reconstructions into compound-encapsulated nanowires, compound-released wires, shortened nanorods or spheres, swollen nanowires, nanorods, and finally branched nanowires/networks. These phase transformations stem from unique environment-labile reaction complexity of the CysMA unit. Such media-sensitive properties provided a versatile tool for the rational design of novel stimuli-responsive materials for biological and other emerging applications.[1-5]

Acknowledgements

This research work was supported by National Natural Science Foundation of China (21274097, 21474069 and 21334004) and the Priority Academic Program Development of Jiangsu Higher Education Institutions.

Notes and references

1 X. Ma and H. Tian, *Acc. Chem. Res.*, 2014, **47**, 1971-1981.
2 P. Theato, B. S. Sumerlin, R. K. O'Reilly and T. H. Epps, III, *Chem. Soc. Rev.*, 2013, **42**, 7055-7056.
3 Z. Ge and S. Liu, *Chem. Soc. Rev.*, 2013, **42**, 7289-7325.
4 E. G. Kelley, J. N. L. Albert, M. O. Sullivan and T. H. Epps, III, *Chem. Soc. Rev.*, 2013, **42**, 7057-7071.
5 Y. Yang and M. W. Urban, *Chem. Soc. Rev.*, 2013, **42**, 7446-7467.
6 A. Doering, W. Birnbaum and D. Kuckling, *Chem. Soc. Rev.*, 2013, **42**, 7391-7420.
7 K. A. Guenay, P. Theato and H.-A. Klok, *J. Polym. Sci., Part A-Polym. Chem.*, 2013, **51**, 1-28.
8 J. Y. Quek, Y. Zhu, P. J. Roth, T. P. Davis and A. B. Lowe, *Macromolecules*, 2013, **46**, 7290-7302.
9 P. Yang, L. P. D. Ratcliffe and S. P. Armes, *Macromolecules*, 2013, **46**, 8545-8556.
10 P. A. Woodfield, Y. Zhu, Y. Pei and P. J. Roth, *Macromolecules*, 2014, **47**, 750-762.
11 X. Wu, H. Zhao, B. Noernberg, P. Theato and G. A. Luinstra, *Macromolecules*, 2014, **47**, 492-497.
12 C. E. Hoyle and C. N. Bowman, *Angew. Chem. Int. Ed.*, 2010, **49**, 1540-1573.
13 C. E. Hoyle, A. B. Lowe and C. N. Bowman, *Chem. Soc. Rev.*, 2010, **39**, 1355-1387.
14 S. Bauhuber, C. Hozsa, M. Breunig and A. Goepferich, *Adv. Mater.*, 2009, **21**, 3286-3306.
15 X. Hu, J. Hu, J. Tian, Z. Ge, G. Zhang, K. Luo and S. Liu, *J. Am. Chem. Soc.*, 2013, **135**, 17617-17629.
16 G. Liu, X. Wang, J. Hu, G. Zhang and S. Liu, *J. Am. Chem. Soc.*, 2014, **136**, 7492-7497.
17 X. Hu, G. Liu, Y. Li, X. Wang and S. Liu, *J. Am. Chem. Soc.*, 2015, **137**, 362-368.
18 Y. Yang, X. Ding and M. W. Urban, *Prog. Polym. Sci.*, 2015. DOI: 10.1016/j.progpolymsci.2015.06.001
19 P. Nowak, V. Saggiomo, F. Salehian, M. Colomb-Delsuc, Y. Han and S. Otto, *Angew. Chem. Int. Ed.*, 2015, **54**, 4192-4197.
20 J. Li, C. Tian, Y. Yuan, Z. Yang, C. Yin, R. Jiang, W. Song, X. Li, X. Lu, L. Zhang, Q. Fan and W. Huang, *Macromolecules*, 2015, **48**, 1017-1025.
21 A. Pal, M. Malakoutikhah, G. Leonetti, M. Tezcan, M. Colomb-Delsuc, V. D. Nguyen, J. van der Gucht and S. Otto, *Angew. Chem. Int. Ed.*, 2015, **54**, 7852–7856.
22 K. D. Zhang and S. Matile, *Angew. Chem. Int. Ed.*, 2015, **54**, 8980–8983.
23 N. Assem, D. J. Ferreira, D. W. Wolan and P. E. Dawson, *Angew. Chem. Int. Ed.*, 2015, **54**, 8665–8668.

24 J. Chang, Y. Tao, B. Wang, B. Guo, H. Xu, Y. Jiang and Y. Huang, *J. Mater. Chem. B*, 2015, **3**, 1097-1105.
25 Q. Zhang, S. Aleksanian, S. M. Noh and J. K. Oh, *Polym. Chem.*, 2013, **4**, 351-359.
26 A. P. Bapat, J. G. Ray, D. A. Savin and B. S. Sumerlin, *Macromolecules*, 2013, **46**, 2188-2198.
27 A. Hall, L. P. Wu, L. Parhamifar and S. M. Moghimi, *Biomacromolecules*, 2015, **16**, 2119–2126
28 S. Quan, Y. Wang, A. Zhou, P. Kumar and R. Narain, *Biomacromolecules*, 2015, **16**, 1978–1986
29 X. Wang, G. Liu, J. Hu, G. Zhang and S. Liu, *Angew. Chem. Int. Ed.*, 2014, **53**, 3138-3142.
30 Y. Anraku, A. Kishimura, M. Oba, Y. Yamasaki and K. Kataoka, *J. Am. Chem. Soc.*, 2010, **132**, 1631-1636.
31 Y. Anraku, A. Kishimura, Y. Yamasaki and K. Kataoka, *J. Am. Chem. Soc.*, 2013, **135**, 1423-1429.
32 K. Bauri, S. G. Roy, S. Pant and P. De, *Langmuir*, 2013, **29**, 2764-2774.
33 X. J. Chen, N. Xu, N. Li, L. C. Lu, Y. L. Cai, Y. Zhao and D. J. Wang, *Soft Matter*, 2013, **9**, 1885-1894.
34 N. Xu, J. Han, Z. Zhu, B. Song, X. Lu and Y. Cai, *Soft Matter*, 2015, **11**, 5546-5553.
35 L. Yuan, J. Liu, J. Wen and H. Zhao, *Langmuir*, 2012, **28**, 11232-11240.
36 J. Chiefari, Y. K. Chong, F. Ercole, J. Krstina, J. Jeffery, T. P. T. Le, R. T. A. Mayadunne, G. F. Meijs, C. L. Moad, G. Moad, E. Rizzardo and S. H. Thang, *Macromolecules*, 1998, **31**, 5559-5562.
37 G. Moad, E. Rizzardo and S. H. Thang, *Acc. Chem. Res.*, 2008, **41**, 1133-1142.
38 J. Rosselgong, A. Blanazs, P. Chambon, M. Williams, M. Semsarilar, J. Madsen, G. Battaglia and S. P. Armes, *ACS Macro Lett.*, 2012, **1**, 1041-1045.
39 A. W. Jackson and D. A. Fulton, *Macromolecules*, 2012, **45**, 2699-2708.
40 G. T. Zugates, D. G. Anderson, S. R. Little, I. E. B. Lawhorn and R. Langer, *J. Am. Chem. Soc.*, 2006, **128**, 12726-12734.
41 C. W. Scales, Y. A. Vasilieva, A. J. Convertine, A. B. Lowe and C. L. McCormick, *Biomacromolecules*, 2005, **6**, 1846-1850.
42 G. Liu, H. Shi, Y. Cui, J. Tong, Y. Zhao, D. Wang and Y. Cai, *Polym. Chem.*, 2013, **4**, 1176-1182.
43 X. W. Xu, A. E. Smith, S. E. Kirkland and C. L. McCormick, *Macromolecules*, 2008, **41**, 8429-8435.
44 B. Bronstert, A. Henne, A. Hesse, M. Jacobi and G. Wallbillich, Patent US 4719297, 1988.
45 J. Z. Du and S. P. Armes, *Langmuir*, 2008, **24**, 13710-13716.
46 E. S. Read, K. L. Thompson and S. P. Armes, *Polym. Chem.*, 2010, **1**, 221-230.
47 Y. Shi, H. Gao, L. C. Lu and Y. L. Cai, *Chem. Commun.*, 2009, 1368-1370.
48 Y. Shi, G. H. Liu, H. Gao, L. C. Lu and Y. L. Cai, *Macromolecules*, 2009, **42**, 3917-3926.
49 J. Y. Tong, Y. Shi, G. H. Liu, T. Huang, N. Xu, Z. G. Zhu and Y. L. Cai, *Macromol. Rapid Commun.*, 2013, **34**, 1827-1832.
50 H. Lin, D. Zhang, P. G. Alexander, G. Yang, J. Tan, A. W. Cheng and R. S. Tuan, *Biomaterials*, 2013, **34**, 331-339.
51 B. D. Fairbanks, M. P. Schwartz, A. E. Halevi, C. R. Nuttelman, C. N. Bowman and K. S. Anseth, *Adv. Mater.*, 2009, **21**, 5005-5010.
52 B. D. Fairbanks, M. P. Schwartz, C. N. Bowman and K. S. Anseth, *Biomaterials*, 2009, **30**, 6702-6707.
53 Y. Y. Jiang, N. Xu, J. Han, Q. P. Yu, L. Guo, P. Gao, X. H. Lu and Y. L. Cai, *Polym. Chem.*, 2015, **6**, 4955-4965.
54 A. B. Lowe and C. L. McCormick, *Prog. Polym. Sci.*, 2007, **32**, 283-351.
55 H. R. Sadik Amajjahe, *Macromolecules*, 2008, **41**, 716-718.
56 V. Jaacks, *Makromol. Chem.*, 1972, **161**, 161-172.
57 B. S. Tucker, S. G. Getchell, M. R. Hill and B. S. Sumerlin, *Polym. Chem.*, 2015, **6**, 4258-4263.
58 R. E. Benesch and R. Benesch, *J. Am. Chem. Soc.*, 1955, **77**, 5877-5881.
59 R. Singh and G. M. Whitesides, *J. Org. Chem.*, 1991, **56**, 2332-2337.
60 G. A. Bagiyan, I. K. Koroleva, N. V. Soroka and A. V. Ufimtsev, *Russ. Chem. Bull.*, 2003, **52**, 1135-1141.
61 A. Mikolajczyk, A. Gajewicz, B. Rasulev, N. Schaeublin, E. Maurer-Gardner, S. Hussain, J. Leszczynski and T. Puzyn, *Chem. Mater.*, 2015, **27**, 2400-2407.
62 S. Sugihara, A. Blanazs, S. P. Armes, A. J. Ryan and A. L. Lewis, *J. Am. Chem. Soc.*, 2011, **133**, 15707-15713.
63 M. Semsarilar, V. Ladmiral, A. Blanazs and S. P. Armes, *Polym. Chem.*, 2014, **5**, 3466-3475.
64 J. R. Lovett, N. J. Warren, L. P. Ratcliffe, M. K. Kocik and S. P. Armes, *Angew. Chem. Int. Ed.*, 2015, **54**, 1279-1283.
65 D. Cavallin, C. De Marco and S. Dupré, *Arch. Biochem. Biophys.*, 1968, **124**, 18-26.
66 A. Hanaki and H. Kamide, *Chem. Pharm. Bull.*, 1975, **23**, 1671-1676.

TOC Graphic

A water-soluble cystamine-block copolymer undergoes air/pH-mediated programmable self-assembly/reconstructions simply stemming from unique environment-labile reaction complexity of the cystamine functionalized unit.